Analyzing And Optimizing The Convective Heat Transfer Coefficient Using Response Surface Methodology For Different Fluids In A Spiral Heat Exchanger

Mehdi Jafari[1,*], Jamshid Khorshidi[2], Ali Sheibani[3], Taleb Zarei[4]

1- *Department of Chemical Engineering, Yazd Branch, Islamic Azad University, Yazd, Iran - me_jafari1984@yahoo.com*
2- *Mechanical Engineering Department, Hormozgan University, Bandar Abbas, Iran - khorshidi@hormozgan.ac.ir*
3- *Department of Chemical Engineering, Yazd Branch, Islamic Azad University, Yazd, Iran - alisheibani@ymail.com*
4- *Chemical Engineering Department, Hormozgan University, Bandar Abbas, Iran - talebzarei@gmail.com*

ABSTRACT

This experimental work deals with the convective heat transfer coefficient (CHTC) optimization in spiral plate heat exchangers (SPHE) by the response surface modeling (RSM). Optimizations were performed utilizing Design of Experiments (DOE) as a product control and optimization tool in the industry. CHTC was optimized by employing different appropriate fluids. The effects of physical properties of fluids, including viscosity, density, and mass flow rate (MFR), on the convective heat transfer factor underwent investigations. The optimized results and the amount of heat power showed an excellent agreement with the SPHE formulation. The experimental results confirmed the direct proportional relationship between the fluid's CHTC and the total heat transfer with its density and MFR, while there was an inverse proportional relationship with the fluid viscosity. Moreover, four semi-empirical linear equations for water, nitrobenzene, ethylene glycol, and oil were obtained from the regression table. The highest and lowest CHTC values were for water and Ethylene Glycol, respectively. As confirmed by the obtained optimal linear equation with the sum of the least squares (R2) with a <10% error and a high accuracy of 90%, the results from the RSM model were accurate.

Keywords: : **Spiral Heat Exchanger, Response Surface Methodology, Design of Experiment , Optimization, Heat Transfer**

1. *INTRODUCTION*

Heat exchangers effectively enable heat exchange between two or more fluids in various fields, including processes and power plants. A spiral heat exchanger has a vital role across different industrial fields. Thanks to low fouling and easy descaling, these heat exchangers could be suitable alternatives to other heat exchanger types in the chemical and food industries, whose processed materials have a lot of sediment. Descaling is one of the cost-effective issues for maintaining heat exchangers and avoiding the waste of capital and time. Heat transfer surface fouling declines the heat transfer rate (HTR) while enhancing pressure drop in heat exchangers. Compact heat exchangers have also attracted much attention recently due to their high efficiency [1].

Spiral plate-type or spiral heat exchangers (SPHEs or SHEs) have two connected stream channels for the production of first and second flow channels to pass the first and second (hot/cold) fluids, respectively. A single metal sheet separates stream channels. The temperature distinction is observable on both channel sides up to *the body periphery. The spacing of the Spiral-formed metallic sheets is at equal distances utilizing spacer studs/spacing pins welded on both sides and providing a uniform cross-sectional area for the fluid flow. These spacer studs allow for the supply of the required thickness of the stream channels. Nickel, stainless steel, nickel, titanium, nickel alloys, carbon steel, and copper alloys are often employed to manufacture SHEs [2].*

SHEs can properly cool slurries and fluids of high viscosity, distinguishing this type of heat exchanger [3]. SHEs are widely applied in condensing or evaporating liquids in various industries, including sugar, paper, and chemicals [4]. The fluid stream temperature throughout the process is critical due to its economic impact. For instance, water evaporation from foods by SHE decreases protein destruction while increasing microbial stability and consequently reducing production capacity and transport costs. Vaporization and dehydration are two crucial issues in dairy ranches. SHE can handle highly viscous liquids with poor fouling propensity [3]. The SHE geometric configuration includes two long plates that are spirally wound. The plates are welded with bolts between them to enhance their mechanical quality [5], providing uniform direction to enable local turbulence changes, stagnation areas elimination, and a self-cleaning channel achievement [3].

Kondhalkar and Kapatkat developed a spiral tube oil extraction apparatus to reduce costs [6]. P. Naphon examined the pressure drop and the heating effectiveness of a helical coil heat exchanger, indicating that the hot and cold liquid MFRs affected heat exchangers' efficacy significantly [7]. M. P. Nueza et al. examined the SHE designs and reported comparatively higher heat transfer rates in SPHEs than other heat exchangers [5]. Egner and Burmeister used computational fluid dynamics (CFD) for the flow behavior analysis along a spiral channel having a rectangular cross-section area, revealing the Nusselt number equation as the spiral's mean diameter function. Moreover, it was found that the Spiral's section had the most extreme heat transfer coefficient (HTC). After the inlet length, HTC was approximately stable, and laminar flow mainly contributed to evaluating the heat penetration depth for flow through spiral (helical) channels. Furthermore, an approximate solution was developed to investigate the thermal efficiency of SHE in thermal parts [8, 9].

Regarding SHE's different shapes, the experimental correlations governing other heat exchangers cannot be employed for the SHE. Minton presented the first equations for the total heat transfer factor and pressure drop calculations under different application modes [11]. Other studies were carried out simultaneously by other researchers to illustrate the relationship between heat transfer and pressure drop. Although most recently published articles on the above subject are based on the results of previous studies, some simplifications and simulations facilitated the use of the correlations and results. Heat exchanger designers investigate the temperature distribution along the heat exchanger path, primarily using the presented method by two professors at the University of Hamburg, T. Bebs and W. Rotzel [23-25]. However, the operating time interval for cleaning is about four times longer than shell and tube heat exchangers. However, the introduced heat exchanger can be easily cleaned and descaled due to easy access to all its surfaces. The SHE has a high thermal efficiency, and the temperature correction factor is very close to 1 [26]. The configuration of heat-exchanging spiral walls allows the starting and ending of the stream channels at the same angle, hence ensuring an identical number of turns represented in Figure 3 [27].

Numerical experiments are performed to examine the interaction of parameters on the HTC (response variable) while determining the optimized HTC for different fluids. Response surface methodology (RSM) simulates the heat transfer coefficient response surface based on numerical experiments and gives a linear model. This study investigates three modeling aspects, Experiment Design, and optimization of SHEs [15, 17, 30]. This paper mainly aimed to discover the optimal equations to achieve optimal heat transfer using suitable fluids without involving the designer in the DOE method and to develop the desired SHE. At first, the SHE was modeled by assuming a constant total HTC and specific heat capacity, followed by the SHE mathematical modeling based on energy balance equations and fluid mechanics.

Moreover, respond surface methodology (RSM) has been utilized for CHTC optimization by Design-Expert software, version 15. To date, no studies have determined the optimal HTC for fluids using the design of experiment optimization approaches, such as RSM. In this study, four fluids suitable for heat transfer in an SHE was selected. We used MATLAB programming and heat transfer and fluid dynamics equations with Design-Expert software for DOE, carried out statistically to find the optimal model of CHTC.

2. *Mathematical Formulations*

2.1.Governing Heat Transfer

The overall heat transfer coefficient or U-value, often used in the design of heat exchangers, is associated with HTR to the fluid's temperature difference. This coefficient covers all resistances of HTR, comprising cold and hot fluid films, wall thickness, and sediment resistance on the hot and cold streams. The heat transfer equation is presented by [1, 28, 29]:

$$Q = m_h C_h (T_{hi} - T_{ho}) = m_c C_c (T_{co} - T_{ci}) \qquad (1)$$

A right prism with a regular hexagonal base construction for fluid movement in the tube around the SHE design is used to achieve maximum heat transfer instead of a cylindrical shape. Many tubes with particular materials are packed in a cylindrical container/bed for certain purposes. If d << D, and you can work with an approximate rather than provably optimal answer, then noncircular-style packing will possibly perform well, enabling the estimation of how many such tubes would fit. Nearly (1/4) of the space is empty from the optimal packing ratio, and more is lost from edge effects because the Hales result highlights the conditions without boundaries. In geometry, close-packing of equal cylindrical tubes represents the congruent cylinders' dense arrangement within an infinite, regular arrangement (or lattice). This typical arrangement can be helpful for optimal volume and minimum occupied space in the industry [29]. The physical principle is based on conserving energy, which means assuming very little heat loss to the environment, leading to equal heat gain and loss of the cold and hot streams, respectively. This study has assessed the entire heat load on the heat exchanger using the thermal equilibrium equation. The U-value is estimated utilizing logarithmic mean temperature difference (LMTD) for pre-defined temperatures at the inlet and output. The heat duty can be determined by [1, 29]:

$$Q = U, A, LMTD \qquad (2)$$

In the above equation, A shows the heat transfer area while F denotes the correction factor and LMTD between the hot and cold fluids. Equation (3) can also be determined as the U-value:

$$U = \frac{1}{\frac{1}{h_h} + \frac{t_w}{K_w} + \frac{1}{h_c} + R_f} \qquad (3)$$

In which, hh and hc, indicate the CHTC of hot and cold fluids, respectively. Kw represents the wall material's conductivity, while Rf stands for the fouling factor. Tw is the wall thickness. Hh and hc can be determined by experimental relations for the Spiral heat transfer [1, 29].

The LMTD is close to 1in this heat exchanger. That is, the flow in this type of heat exchanger resembles the actual reverse flow. The overall HTC of this heat exchanger has higher values than obtained for the shell and tube ones, implying the SHE's small size. LMTD can be determined by Eq. (4) [1, 28, 29].

$$LMTD = \frac{(T_{hi} - T_{co}) - (T_{ho} - T_{ci})}{Ln(\frac{T_{hi} - T_{co}}{T_{ho} - T_{ci}})} \qquad (4)$$

The following expressions are utilized to estimate the heat transfer area and Nusselt number:

$$A = 2 * L * H \qquad (5)$$

$$Nu = 0{,}239 \left(1 + 5{,}54 \frac{D_H}{R_m}\right) Re^{0{,}806} Pr^{0{,}268} \qquad (6)$$

Equation (6) calculates the Nusselt number derived from the Reynolds (Re) and Prandtl (Pr) numbers, which can evaluate the HTC. Rm and DH represent the heat exchanger's mean diameter and the hydraulic diameter, respectively. The following represents an expression for the Reynolds number regarding mass flow (M).

$$Re = M, \frac{D_H}{\mu} \qquad (7)$$

In the above equation, Eqs. (8) and (11) can be utilized to determine the fluid's mean velocity (v) and the Prandtl number (Pr). P, ṁ, and k denote the fluid density, MFR, and thermal conductivity, respectively [1, 29].

$$v = \frac{\dot{m}}{\rho A} \qquad (8)$$

$$M = \frac{m}{A_C} \tag{9}$$

The mean radius is calculated as follows:

$$R_m = \frac{R_{min}+R_{max}}{2} \tag{10}$$

The Prandtl number can be evaluated according to the stream's physical characteristics through the equation below:

$$Pr = \frac{C_P \mu}{k} \tag{11}$$

It is possible to calculate the HTC by estimating the Nusselt number using the Reynolds and Prandtl values as a starting point.

$$h = \frac{k,Nu}{D_h} \tag{12}$$

2.2.Pressure drops in SPHE

The below equation can be used to calculate the pressure drop in both streams and the SHE's external diameter [1, 29].

$$\Delta P = \frac{1{,}45(L,v^2\rho)}{1{,}705} \tag{13}$$

Where, v shows the velocity, and ρ is the density of the fluid.

3. Problem Description

3.1.Design procedure

The fluid stream, heat transfer characteristics, and the designated hot and cold flow rates were all considered when modeling a SHE (Table 1). The cold and hot fluids had stable inlet temperatures, while their outlet temperatures were determined for counter-flow arrangement.

An SHE was employed to cool three various hot fluids with a 0.5-1 (kg/s) mass flow rate. The water-cooling fluid enters the heat exchanger at a 0.5 kg/s flow rate, which must be heated from 32.87°C. The fouling factor is 0.00017 m2.C/W. Stainless steel makes up the heat exchanger's wall. The appropriate heat exchanger was selected according to the physical characteristics of cold and hot fluids, according to Figure 4.

Table 1. *Characteristics of SPHE.*

Parameters	**Values**
Height (plate width) (m)	0.457
Plate length (m)	2.515
Spiral diameter (m)	0.304
Channel spacing (m)	0.00635
Heat transfer area (m2)	3.49
Thickness of the plate (m)	0.001
The material of the plate	Stainless steel
Stainless steel heat *conductivity (W/m.C)*	14
Number of turns (pass)	7

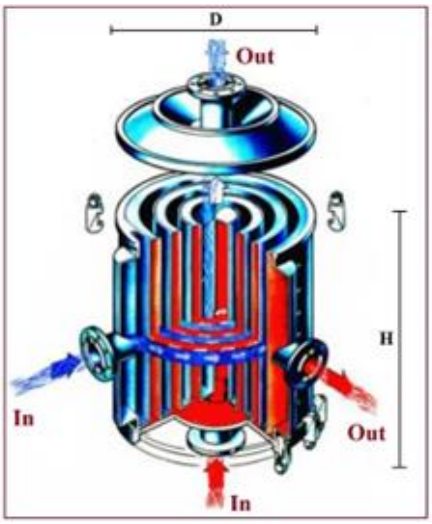

Fig. 1. *Geometrical features of the modeled SPHE.*

4. Materials and Methods

Four fluids (water, nitrobenzene, ethylene glycol, and a standard oil) were selected as working fluids in this heat exchanger to optimize the CHTC formula. Then, each fluid's temperature in the SHE was measured. The heat transfer amount Q (J/s) and the CHTC h (W/m2.C) are a function of MFR (kg/s), density (kg/m3), and viscosity (N.s/m2) of the fluid. The low and high temperatures were chosen as the minimum and maximum levels, and the average level was obtained by dividing the sum of the two temperatures as follows.

$$T_{avg} = \frac{T_{min}+T_{max}}{2} \quad (14)$$

4.1.Process Performance

The physical properties of four fluids (viscosity and density) and mass flow rate in the SHE tube were determined for all three high, medium, and low-temperature levels. Several different cases were selected to measure fluid properties by the RSM method, in which the physical properties and fluid velocity are independent parameters (factors), and the heat transfer coefficient is the dependent parameter (response).

4.2.Experimental Design

In the Design-Expert software, the maximum (+1), middle (0), and minimum (-1) level were specified as coded values (-1, 0, +1), and the number of different states in the design of experiment (DOE) was determined. The physical properties at various levels were determined in each test, and the responses, HTR (Q), and CHTC (h) were entered into the software after calculations.

An optimal equation for each fluid was obtained to discover the convective heat transfer factor and the fluid type effects on HTR. Table 2 indicates values obtained for different variable levels for density, viscosity, and MFR for water, nitrobenzene, ethylene glycol, and industrial oil fluids.

Table 2. *Absolute and coded values for the variables in each fluid*

Water			
$\rho\ (\frac{kg}{m3})$	975	982.5	990
$\dot{m}\ (\frac{kg}{s})$	0.5	0.75	1
$\mu\ (pa, s)$	0.000547	0.000691	0.00089
Coded Value	-1	0	+1

Nitrobenzene			
$\rho\ (\frac{kg}{m3})$	1110	1151	1192
$\dot{m}\ (\frac{kg}{s})$	0.5	0.75	1
$\mu\ (pa, s)$	0.0018	0.00185	0.0019
Coded Value	-1	0	+1

Ethylene glycol			
$\rho\ (\frac{kg}{m3})$	1055	1071	1087
$\dot{m}\ (\frac{kg}{s})$	0.5	0.75	1
$\mu\ (pa, s)$	0.0031	0.0066	0.011
Coded Value	-1	0	+1

Standard Oil			
$\rho\ (\frac{kg}{m3})$	841	855	870
$\dot{m}\ (\frac{kg}{s})$	0.5	0.75	1
$\mu\ (pa, s)$	0.0016	0.0024	0.0045
Coded Value	-1	0	+1

Table 3 reports the design of experiments, including three factors and levels considered for 20 runs. RSM was characterized utilizing Design-Expert, and RSM analyses were employed to optimize the experimental factors more effectively and to illustrate the essential factor interactions. In Table 3, the different values of the tested variables by the RSM method and their responses for 20 modes, some of which were repeated (0, 0, 0), were given to increase accuracy. Various experiments for determining the heat transfer coefficient (h) were provided for four fluids, including water, nitrobenzene, ethylene glycol, and a standard oil, in various situations.

Table 3. *Design of the experiment and responses (h, Q)*

N	ρ	$\dot{m}$	μ	hwater	hNitro	hGlycol	hOil	Q
1	1	1	-1	838440	15255	9875.4	16763	104500
2	0	0	0	552500	14925	5395.2	12119	78375
3	0	0	0	552500	14925	5395.2	12119	78375
4	0	-1	0	399440	10790	3900	8762	52250
5	1	-1	-1	481560	11029	7139	12119	52250
6	0	0	-1	666070	15255	9875	16763	78375
7	1	-1	1	326230	10563	2592	5299	52250
8	1	0	0	552500	14925	3585	7329	78375
9	0	0	0	552500	14925	5395.2	12119	78375
10	-1	-1	1	399440	8762	8762	8762	52250
11	-1	0	0	695470	14925	5395	12119	104500
12	1	1	1	567000	18390	4513	9226	104500
13	-1	1	-1	568000	19203	12431	21101	52250
14	0	0	1	451230	14610	3585	7329	78375
15	0	1	0	695470	18787	6791	15255	104500
16	0	0	0	552500	14925	5395.2	12119	78375
17	0	0	0	552500	14925	5395.2	12119	78375
18	0	0	0	552500	14925	5395.2	12119	78375
19	-1	-1	-1	481560	11029	7139	12119	52250
20	-1	1	1	568000	18390	4513	1462	52250

5. *Results and Discussion*

5.1. CHTC Optimization Results

The optimal equation of four different fluids was calculated utilizing water (R1) (Table 4) as cold fluid, nitrobenzene (R2) (Table 5), ethylene glycol (R3) (Table 6), and standard industrial oil (R4) *(Table 7) for heating in the SHE, as variables or factors in Design-Expert. The results or responses were entered in the software for 20 different modes with the RSM, highlighting the optimal relationship* *among standard and variance tables (ANOVA) and the model type (linear, non-linear, and power model) for the best mode.*

Optimization results for different fluids were reviewed in this section. In these calculations, closer values of the minimum square error (R2) to 1 show higher accuracy of the calculations, and the negative values are invalid. Also, P-values of <0.05 will show significance, and higher F values will represent more accurate results. The lower the parameter of the model's lack of fit (LF), the better, and lower values of this parameter show that the model is more suitable for choosing the optimal relationship. In addition to these essential parameters in the analysis of variance or standard deviation table, all the parameters of the optimal model were checked for different variables while also examining the interaction or effect of variables on each other or individually in the optimal relationship, along with residual values, error, least squares, and P- and F-values, which are all statistical parameters in the model analysis. In these calculations, A, B, and C are the physical properties of fluids, namely density (A), velocity (B), and viscosity (C). In the RSM method, the interaction model of two coefficients or factors (2FI) was used to reduce the number of calculations and ensure less error.

According to Tables 4 to 7, the linear model with appropriate p values can be selected with the highest accuracy (R2) for the tested fluids in this work.

Table 4. *Choosing the fit model for the optimal equation for water.*

Source	Sequential p-value	LF p-value	Adjusted R2	Predicted R2	
Linear	<0.0001		0.6950	0.5236	Suggested
2FI	0.0432		0.7950	0.3800	Suggested
Quadratic	0.5181		0.7855	0.1135	
Cubic	0.0635		0.9031	-5.7466	Aliased

Table 5. *Choosing the fit model for the optimal equation for Nitrobenzene.*

Source	Sequential p-value	LF p-value	Adjusted R2	Predicted R2	
Linear	<0.0001		0.8383	0.7500	Suggested
2FI	0.0179		0.9060	0.6882	Suggested
Quadratic	0.7141		0.8927	0.5659	
Cubic	0.0392		0.9592	-1.8367	Aliased

Table 6. *Choosing the fit model for the optimal equation for ethylene glycol.*

Source	Sequential p-value	LF p-value	Adjusted R2	Predicted R2	
Linear	<0.0018		0.5244	0.2804	Suggested
2FI	0.0952		0.6351	-0.4099	Suggested
Quadratic	0.2581		0.6773	-0.4233	
Cubic	0.0659		0.8522	-9.2894	Aliased

Table 7. *Choosing the fit model for the optimal equation for standard oil.*

Source	Sequential p-value	LF p-value	Adjusted R2	Predicted R2	
Linear	0.0002		0.6463	0.4469	Suggested
2FI	0.0239		0.7842	0.0216	Suggested
Quadratic	0.9006		0.7346	-0.1996	
Cubic	0.0033		0.9576	-1.9523	Aliased

5.2.ANOVA for Experiments

ANOVA is a valuable tool that improves DOE analysis and complements the results. The ANOVA results for CHT (h) are displayed in Tables 8 through 11. The degree of freedom (DF), the adjusted R2 (Adj SS), sequential SS or Seq SS (R2), and the F-value appear in the ANOVA table when we perform a regression analysis or an ANOVA statistical examination to control whether the means of two populations differ considerably. Additionally, the F test will indicate whether or not a set of variables is jointly significant. The F-value can be used to determine the possibility of accepting or rejecting the null hypothesis. The p-value must be additionally taken into account, considering that what determines its value is the F-value, and the influential variables are detected using the two values together. It should be noted that all of our variables are not significant even if we have a considerable F-value.

The statistic compares the combined effects of all the factors. The P-values should be examined separately to see which variables are statistically substantial for p values less than the alpha threshold. Otherwise, our findings would not be noteworthy, and the null hypothesis could not be ruled out. Tests typically have an alpha level of 0.05. As indicated by the p-value, the sample results can be likely under a true null hypothesis. P-values are between 0 and 1, with smaller values ($P<0.05$), a widely accepted significance threshold, indicating that each rate is statistically affected by the power level. The response is significantly influenced by all three variables: mass flow rate ($\dot{m}$), density (ρ), and viscosity (μ), as indicated by the data in column P. Thus, the p-value for the factors and MFR interactions shows higher significance, and the also value of $\dot{m}$ for the CHT result (h). Therefore, the fluid's MFR directly affects the CHT (h), and the CHT and fluid viscosity are inversely related.

Since the MFR F-value in the ANOVA table shows the lowest in column F, an increase in viscosity consequently decreases in CHT on the heat exchanger. Additionally, the R2 value demonstrates that MFR imposes more significant impacts than the fluid viscosity and velocity.

The F-value and R2 confirm the experimental results and highlight the experimental model's significance. The mean squares (MS) display the precision of the results. Additionally, the experimental data and the ANOVA results for the R2 and F-value in the relevant columns show good consistency.

According to Table 8, an F-value equal to 17.08 shows the model's acceptability, indicating only a 0.01% likelihood of disturbing effects for a large F-value. A P-value of <0.05 highlights acceptability of the model's terms. Here, terms of mass flow rate (A), velocity (B), and viscosity (C) of the fluid alone and on the interactions of density-velocity (AB) and density-viscosity (AC), in the optimal equation for the CHTC (h) of the water are essential in the ANOVA table. Moreover, p value of >0.1 indicate insignificance of this parameter. Therefore, a linear equation with fewer parameters can improve the model.

Table 8. *ANOVA results according to two coefficients' interaction model for water.*

Source	SS	df	Mean Square	F-value	p-value	Equation
Model	2.187E+11	5	4.373E+10	17.08	<0.0001	significant
A-A	1.432E+08	1	1.432E+08	0.0559	0.8165	
B-B	1.336E+11	1	1.336E+11	52.17	<0.0001	
C-C	5.545E+10	1	5.545E+10	21.66	0.0004	

AB	1.468E+10	1	1.468E+10	5.73	0.0312	
AC	1.485E+10	1	1.485E+10	5.80	0.0304	
Residual	3.584E+10	14	2.560E+09			
Lack of Fit	3.584E+10	9	3.982E+09			
Pure Error (PE)	0.0000	5	0.0000			
Cor Total	2.545E+11	19				

According to Table 9, the F-value of 31.51 confirms acceptability of the model, indicating only a 0.01% likelihood of disturbing effects for a large F-value. Here, velocity (B), density-velocity (AB), and density-viscosity (AC) interactions are essential in the optimal relation for the CHTC (h) of the Nitrobenzene. In the ANOVA table, p values of >0.1 show that it is not an important parameter. Therefore, a linear equation with fewer parameters can improve the model.

Table 9. *ANOVA results according to the interaction model of two coefficients for Nitrobenzene.*

Source	SS	df	Mean Square	F-value	p-value	Equation
Model	1.493E+08	6	2.488E+07	31.51	<0.0001	significant
A-A	3.375E+05	1	3.375E+05	0.4275	0.5246	
B-B	1.373E+08	1	1.373E+08	173.91	<0.0001	
C-C	1.638E+05	1	1.638E+05	0.2075	0.6563	
AB	4.131E+06	1	4.131E+06	5.23	0.0396	
AC	4.131E+06	1	4.131E+06	5.23	0.0396	
BC	3.194E+06	1	3.194E+06	4.05	0.0655	
Residual	1.026E+07	13	7.896E+05			
Lack of Fit	1.026E+07	8	1.283E+06			
PE	0.0000	5	0.0000			
Cor Total	1.595E+08	19				

The F-value of 7.98 confirms acceptability of the model (Table 10), indicating only a 0.18% likelihood that a large F-value will cause a nuisance. Hence, viscosity (C) in the optimal equation for the ethylene glycol convective heat transfer coefficient (h) is essential. Therefore, a linear relationship with fewer parameters can improve the model.

Table 10. *ANOVA results according to the interaction model of two coefficients for ethylene glycol.*

Source	SS	df	Mean Square	F-value	p-value	Equation
Model	6.627E+07	3	2.209E+07	7.98	0.0018	significant
A-A	5.575E+06	1	5.575E+06	2.02	0.1749	
B-B	8.169E+06	1	8.169E+06	2.95	0.1050	
C-C	5.252E+07	1	5.252E+07	18.99	0.0005	

Residual	4.426E+07	16	2.767E+06
Lack of Fit	4.426E+07	11	4.024E+06
PE	0.0000	5	0.0000
Cor Total	1.105E+08	19	

According to Table 11, the F-value of 12.51 confirms acceptability of the model, indicating only a 0.18% likelihood of disturbing effects for a large F-value. Here, the variable viscosity (C), velocity (B), and velocity-viscosity interaction (BC) are essential in the optimal relationship for the CHTC (h) for standard oil. Therefore, a linear equation with fewer parameters can enhance the model.

Table 11. *ANOVA results according to the interaction model of two coefficients for standard oil.*

Source	SS	df	Mean Square	F-value	p-value	Equation
Model	2.916E+08	6	4.860E+07	12.51	<0.0001	significant
A-A	100.24	1	100.24	0.0000	0.9960	
B-B	3.283E+07	1	3.283E+07	8.45	0.0122	
C-C	2.074E+08	1	2.074E+08	53.38	<0.0001	
AB	5.932E+06	1	5.932E+06	1.53	0.2384	
AC	9.329E+06	1	9.329E+06	2.40	0.1452	
BC	3.612E+07	1	3.612E+07	9.30	0.0093	
Residual	5.051E+07	13	3.885E+06			
Lack of Fit	5.051E+07	8	6.313E+06			
PE	0.0000	5	0.0000			
Cor Total	3.421E+08	19				

5.3.DOE Analysis

Outcomes of P-values were considered a criterion for comprehending the model's significance, as shown in ANOVA Tables. The model has more significance when the values of P are smaller. P-values of >0.05 showed insignificance and lack of contribution. The half-normal probability plots were considered while choosing the factors and their interactions that had the most remarkable effects.

5.4.Regression Analysis

Tables 12 to 15 provide regression coefficients, standard error (SE), and T- and P-values in the whole linear models for convective heat transfer. A, B, and C represent the density (kg/m3), the velocity (m/s), and the fluid's viscosity (pa.s), respectively, in each regression table.

It is more appropriate to use the fitted linear model or first-order polynomial. Regression analyses were conducted on the experimental data under regression tables, and the linear equation predicted by the model for maximum heat transfer was used to identify the total CHTC for each fluid. The P and T-values must be ascertained to perform the significance test of each model coefficient. The T-value indicates the importance considered for the influence of independent variables on the response value.

According to the P-value, the response is statistically significantly impacted by the three primary components and two interactions. Thus, the optimal equations can be shortened by ignoring specific elements *in the linear equation of the CHTC for each fluid. Such effects on the response (h) show less significance for p-values of >0.05.*

According to Regression tables for the optimized CHTC (h) calculation for each fluid (water, nitrobenzene, ethylene glycol, and standard oil) and considering each change in the response in terms of the changes in the variable's value, the coefficients of the equation are estimated while keeping all the factors constant. Interpolating an orthogonal design yields an overall mean response for all runs. Coefficient adjustment is performed near average values according to factor settings. If the coefficients are orthogonal, the variance inflation factor (VIF) is 1. VIFs higher than one indicate multicollinearity, and higher VIF values indicate a strong equation for the factors. As an essential rule, VIFs above 10 are acceptable. In addition, the confidence interval (CI) or confidence level (1-α) is calculated from the probability of type error 1, which is also called the test level, represented by α. The higher the confidence interval in the regression tables, the higher the accuracy of the statistical results.

Table 12. *Regression results for the estimated coefficients for water.*

Factors	Coefficient Estimates	df	SE	95% CI Low	95% CI High	VIF
Intercept	5.503E+05	1	11313.49	5.260E+05	5.745E+05	
A-A	-3237.64	1	13691.04	-32601.99	26126.72	1.0000
B-B	98888.89	1	13691.04	69524.53	1.283E+05	1.0000
C-C	-63719.39	1	13691.04	-93083.74	-34355.03	1.0000
AB	42831.25	1	17888.20	4464.87	81197.63	1.0000
AC	-43081.25	1	17888.20	-81447.63	-4714.87	1.0000

According to the coefficient estimation regression tables, the optimal equation for the CHTC was calculated by analyzing the response surface method for each fluid. The equation, in the form of real coefficients, can predict the response for each factor's desired levels. In this case, the levels (maximum, minimum, and average value) must be defined as actual physical units (SI) for each variable according to the fluid temperature instead of the coded value in the software (-1, 0, and +1) and should be included in the equation. This relation is a semi-empirical equation derived from the linear model and is not applicable in determining the relative impact of each variable, as it is scaled to match the units of each variable.

Table 13. *Regression results for the estimated coefficients for nitrobenzene.*

Factors	Coefficient Estimates	df	SE	95% CI Low	95% CI High	VIF
Intercept	14573.15	1	198.69	14143.91	15002.39	
A-A	-157.21	1	240.44	-676.66	362.24	1.0000
B-B	3170.88	1	240.44	2651.43	3690.33	1.0000
C-C	-109.52	1	240.44	-628.97	409.92	1.0000
AB	-718.63	1	314.16	-1397.32	-39.93	1.0000
AC	718.62	1	314.16	39.93	1397.32	1.0000
BC	631.87	1	314.16	-46.82	1310.57	1.0000

Table 14. *Regression results for the estimated coefficients for ethylene glycol.*

Factors	Coefficient Estimates	df	SE	95% CI Low	95% CI High	VIF
Intercept	6213.75	1	371.92	5425.31	7002.19	
A-A	-638.95	1	450.08	-1593.08	315.18	1.0000
B-B	773.39	1	450.08	-180.74	1727.52	1.0000
C-C	-1961.10	1	450.08	-2915.23	-1006.97	1.0000

Table 15. *Regression results for the estimated coefficients for standard oil.*

Factors	Coefficient Estimates	df	SE	95% CI Low	95% CI High	VIF
Intercept	11595.60	1	440.74	10643.43	12547.77	
A-A	-2.71	1	533.37	-1154.98	1149.56	1.0000
B-B	1550.35	1	533.37	398.08	2702.62	1.0000
C-C	-3896.87	1	533.37	-5049.14	-2744.60	1.0000
AB	861.12	1	696.88	-644.39	2366.64	1.0000
AC	1079.88	1	696.88	-425.64	2585.39	1.0000
BC	-2124.88	1	696.88	-3630.39	-619.36	1.0000

From the regression tables to estimate the coefficients, four semi-empirical linear equations were obtained for water, nitrobenzene, ethylene glycol, and oil, respectively. After reducing the model to a linear form, all of the effects (interaction and first-order) were still significant (P<0.05). As a result, the following equations were obtained.

$$h_{Water} = +5{,}5 * 10^{5} - 3237{,}635\rho + 98888{,}8V - 63719{,}3\mu + 42831{,}25\rho V - 43081{,}25\rho\mu \quad (14)$$

$$h_{NB} = 14573{,}15 - 157{,}21\rho + 3170{,}88V - 109{,}52\mu - 718{,}63\rho V + 718{,}62\rho\mu + 631{,}87V\mu \quad (15)$$

$$h_{EG} = 6213{,}75 - 638{,}95\rho + 773{,}39V - 1961{,}1\mu \quad (16)$$

$$h_{Oil} = 11595{,}6 - 2{,}71\rho + 1550{,}35V - 3896{,}87\mu + 861{,}12\rho V + 1079{,}88\rho\mu - 2124{,}88V\mu \quad (17)$$

According to contour diagram 2, with increasing fluid density and decreasing velocity, the CHTC and fluid Nusselt number increase, and the optimal area is in the blue area at the bottom right of the diagram.

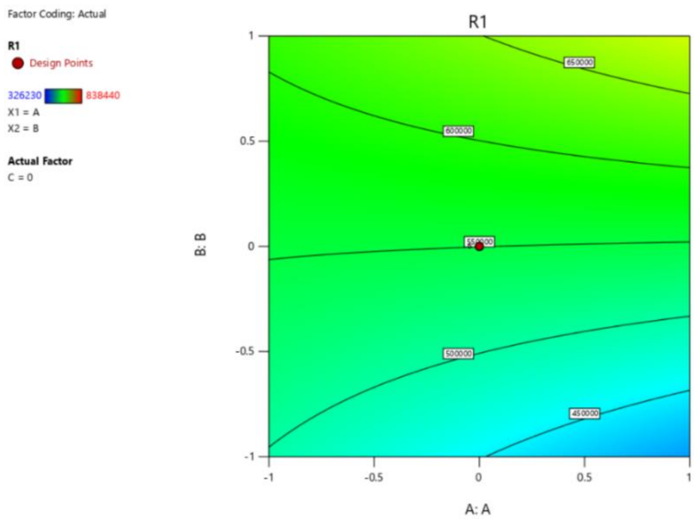

Fig. 2. *Contour plot of the Influence of density (A) and velocity (V) parameters on CHTC of water (R1).*

Figure 3 shows the ratio of the predicted points to the actual values for the HTC, highlighting the corresponding points for each test predicted by the software with the optimal equation.

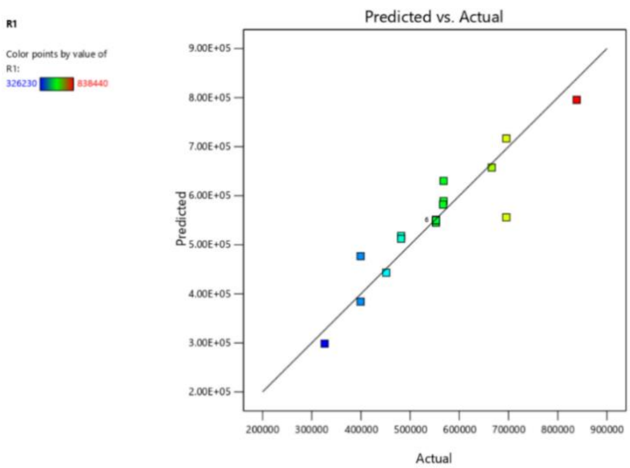

Fig. 3. *Graph of the ratio of values predicted by the software to the actual value for water.*

According to contour diagram 4, as the fluid density increases and velocity decreases, the CHTC and Nusselt number of the fluid increase, and the optimal area is in the blue area at the bottom of the diagram on the right.

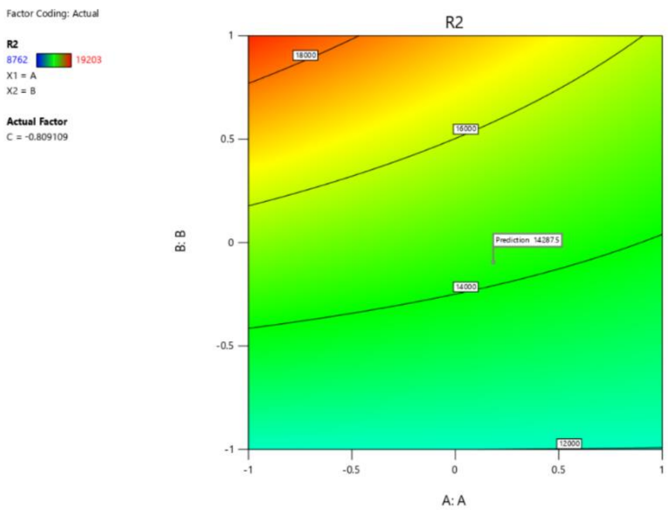

Fig. 4. *Contour plot of interaction data for velocity (B) and density (A) on convective heat transfer coefficient of nitrobenzene (R2).*

Figure 5 shows the ratio of predicted points to actual values or points for the HTC and the corresponding points predicted by the software with the optimal relationship for each test. In this diagram, it is enough to draw a perpendicular line from the desired point on each axis and then read the corresponding value.

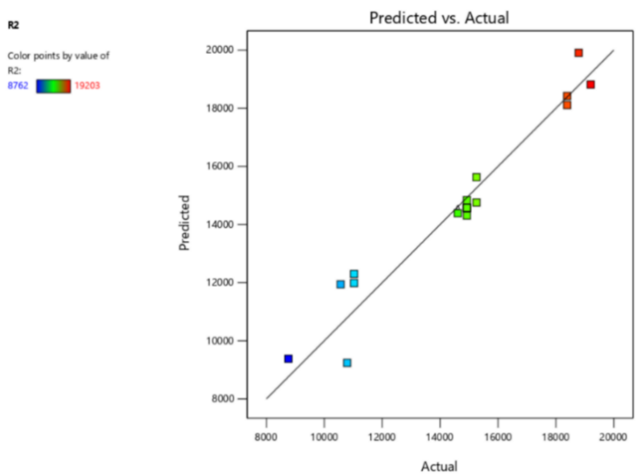

Fig. 5. *Graph of the ratio of the values predicted by the software to the actual values for nitrobenzene.*

According to contour diagram 6, with increasing fluid density and decreasing velocity, the HTC and fluid Nusselt number increase, and the optimal area is in the blue area at the bottom right of the diagram.

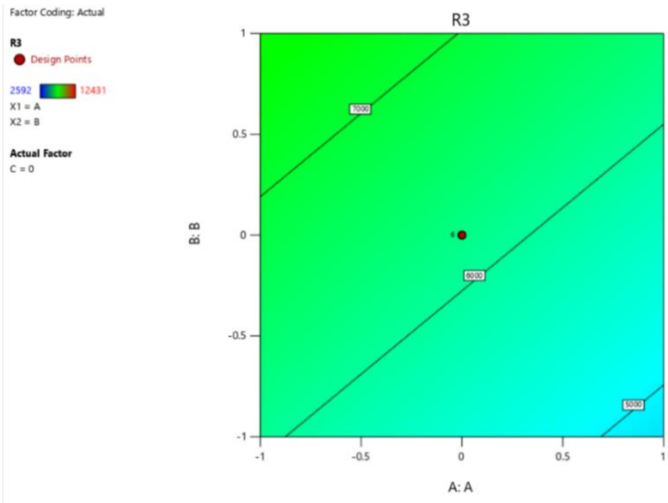

Fig. 6. *Contour plot of the velocity (B) and density (A) interaction on convective heat transfer coefficient of ethylene glycol (R3).*

Figure 7 represents the ratio of predicted points to real values or points for the CHTC and the predicted corresponding point by the software with the optimal equation for each test. In this diagram, it is enough to draw a perpendicular line from the desired point on each axis and then read the corresponding value.

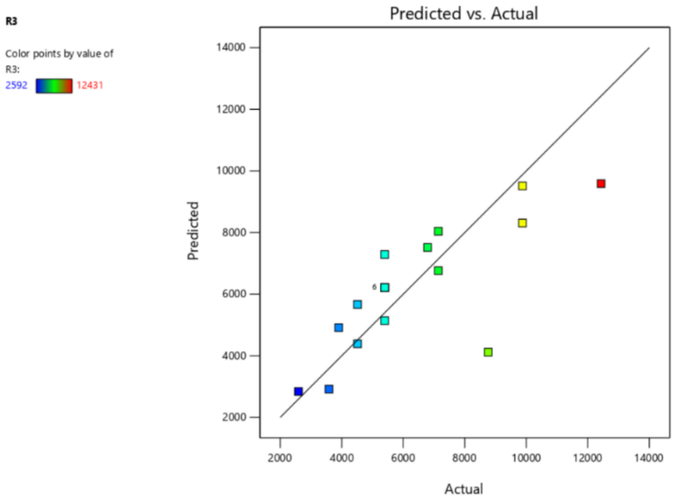

Fig. 7. *Graph of the ratio of the values predicted by the software to the actual values for ethylene glycol.*

According to contour diagram 8, with increasing fluid density and decreasing velocity, the CHTC and fluid Nusselt number increase, and the optimal area is in the blue area at the bottom right of the diagram.

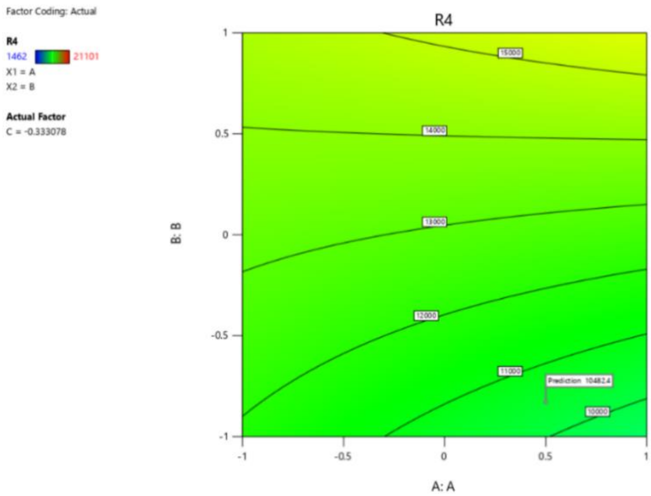

Fig. 8. *Contour diagram of the interaction effect of variables for Velocity (B) and density (A) on convective heat transfer coefficient of oil (R4).*

Diagram 9 shows the ratio of predicted points to actual values or points for the HTC and the indicated corresponding points by the software with the optimal relationship for each test. In this diagram, it is enough to draw a perpendicular line from the desired point on each axis and then read the corresponding value.

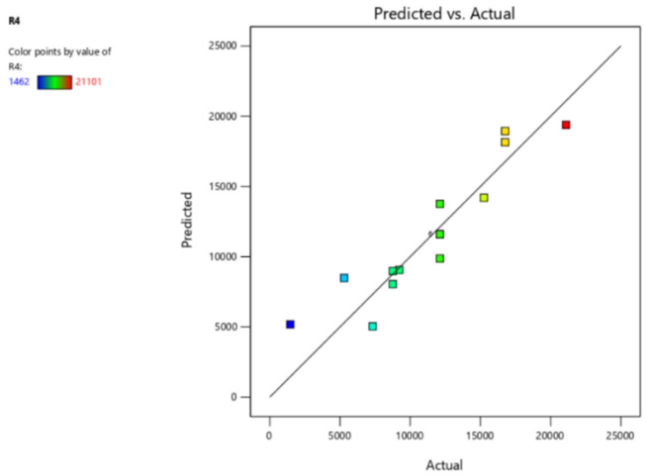

Fig. 9. *Graph of the ratio of the values predicted by the software to the actual values for the oil.*

5.5. Validation of the RSM Model

Four optimal equations for convective heat transfer coefficient (h) for water, nitrobenzene, ethylene glycol, and oil were obtained by examining heat transfer responses in 20 different modes with response surface method and Design Expert software. As it is clear from the optimal relationships and Table 3, the highest and the lowest HTCs are for water and ethylene glycol, respectively. The HTC values for nitrobenzene are almost close to the oil but lower than water because of water's high heat capacity, revealing the accuracy of the response surface method. According to Table 3, modes number 20 and 11 have the lowest and the highest values for HTC, respectively, and number 7 has the second value for HTC. As shown by these results, the influence of fluid density, velocity, and viscosity parameters on the CHTC has the *linear model. Fluid velocity directly impacts the HTC, and density is the most effective next factor. The speed and the fluid viscosity have respective positive and negative and decreasing impacts on the HTC of the fluid, respectively. Therefore, we will have the highest HTC values by increasing the density and decreasing the viscosity.*

The CHTC data and the ANOVA table were used for the regression model's significance test, and the anticipated model underwent validation to examine the model's suitability for future use. Table 3 shows a reasonable match between the expected values and the experimental data, indicating the model's strong generalization ability and prediction accuracy. Most of the data in the regression tables have a confidence interval (CI) greater than 95%, indicating the accuracy of the RSM model's predictions. Also, a 95% upper confidence interval (CI) represents a range of values (upper and lower) with potential 95% confidence, the true mean of the results. The optimal linear equation was obtained as the best model by using the optimal statistical parameters F-value and P-value and the sum of the least squares (R2) with an error of <10% and contributed to calculating the optimal CHTC in the SHE, and the surface response method had a high accuracy of 90%.

6. Conclusions

This research sought to present a systematic and up-to-date examination of the Spiral heat exchanger (SHE) and its optimization by RSM. This approach was utilized to check and find the optimal relationship of the CHTC for four different fluids while investigating the effect of fluid parameters, speed, density, and viscosity on the optimal equation. Design Expert software calculated the optimal HTC, which was a function of the fluid's density, velocity, and viscosity, highlighting that the liquid's density and speed had a positive effect on the HTC. Still, the viscosity reduces the HTC. Also, the highest HTC was for water, and the lowest was for ethylene glycol. From the regression tables to estimate the coefficients, four semi-empirical linear equations were obtained for water, nitrobenzene, ethylene glycol, and oil, respectively.

Investigations were performed to find out how the essential variables would affect the fluid heat transfer. As shown by the RSM results, the MFR of each fluid showed direct proportion to the CHTC and inverse associations with the fluid viscosity. Significance tests of the regression model were performed employing the ANOVA table and CHTC findings. Validation of the predicted model aimed to assess the model's suitability for future use. The expected values and the experimental data are in reasonably good agreement and confirm the excellent predictive accuracy and the model generalization ability. The confidence intervals (CI) are more significant than 95% for most of the data in the regression table, indicating the accuracy of the RSM model results. The 95% upper confidence interval (CI) represents the range of values (upper and lower values) for which you can be 95% certain. The actual mean value of results was obtained using the optimal statistical parameters F and P values and least sum of squares (R2), the optimal linear equation with <10% error as the best model, and used to calculate the optimal convection. The SHE and RSM coefficients have a high accuracy of 90%.

The heat exchanger's heat transfer was improved when the physical conditions were optimized for the operational factors. The RSM design revealed the CHTC's considerable first-order impacts. Entering the values obtained for independent variables into the regression model formula confirmed the model's validity. As shown, the fluid's MFR affected convective heat transfer more than the other variables. In conclusion, choosing the right processing conditions can significantly lower thermal losses. The pressure drops along the SHE and temperature variations can be the subject of future investigation. Additionally, RSM might be a helpful tool for designing a SHE in the best possible way. These can result in the following conclusions:

RSM can be a robust statistical method for optimization, providing the most accurate and optimal answer, according to the table of variance and standard deviation.

The numerical method is an economic way to select the ideal fluid system for SHEs.

RSM is an accurate statistical method with the slightest error for calculating an optimal relationship.

7. References

[1] *Sabouri Shirazi A, Jafari Nasr M, Ghodrat M, 2020. Effects of temperature differences in optimization of spiral plate heat exchangers. PIOS 4: 391-408. https://link.springer.com/article/10.1007/s41660-020-00128-5*

[2] Pradeep Mohan Kumar K, Vijayan V, Suresh Kumar B, et al., 2018. Computational analysis and optimization of spiral plate heat exchanger. JAFM 11: 121-128. DIO: 10.36884/JAFM.11.SI.29428

[3] Azad AV, Amidpour M, 2011. Economic optimization of shell and tube heat exchanger based on constructal theory. Energy 36: 1087-1096. https://doi.org/10.1016/j.energy.2010.11.041

[4] Moretta AA, 2010. Spiral plate heat exchangers: sizing units for cooling non-Newtonian slurries: this article presents step-by-step guidance to demystify the sizing of these exchangers. Chem. Eng. 117: 44-50.

[5] Picón-Núñez M, Canizalez-Dávalos L, Martínez-Rodríguez G, et al., 2007. Shortcut design approach for spiral heat exchangers. Food Bioproducts Processing 85: 322-327. https://doi.org/10.1205/fbp07073

[6] Kondhalkar G, Kapatkat V, 2012. Performance Analysis of Spiral Tube Heat Exchanger used in oil extraction system. IJMER 2: 930-936.

[7] Naphon P, 2007. Thermal performance and pressure drop of the helical-coil heat exchangers with and without helically crimped fins. ICHMT 34: 321-330. https://doi.org/10.1016/j.icheatmasstransfer.2006.11.00

[8] Egner MW, Burmeister LC, 2005. Heat transfer for laminar flow in spiral ducts of rectangular cross section. Heat Transfer 127: 352-356. https://doi.org/10.1115/1.1857950

[9] Burmeister LC, 2006. Effectiveness of a spiral-plate heat exchanger with equal capacitance rates. https://doi.org/10.1115/1.2150839

[10] Rao KR., 1991. Optimal Synthesis of Shell and Tube Heat Exchangers.

[11] Minton P, 1970. Designing Spiral Plate Exchangers. Chem. Eng. Progr. 11: 103-112.

[12] Martin H, 1992. Heat Exchangers (1st Ed.). In: Corporation HP (ed). NewYork: Routledge, 73-82.

[13] Ghodrati M, Khorshidi J, 2021. New experimental Nusselt number correlation for spiral plate heat exchanger optimized using a code. Part A: J. Power and Energy 235: 1142-1158. https://doi.org/10.1177/0957650920948296

[14] Dongwu W, 2003. Geometric calculations for the spiral heat exchanger. Chem. Eng. Technol. Chem. Eng. Technol: Industrial Chemistry-Plant Equipment-Process Engineering-Biotechnology 26: 592-598. https://doi.org/10.1002/ceat.200390091

[15] Antony J, 2023. Design of experiments for engineers and scientists: Elsevier. https://books.google.com

[16] Diamond WJ, 2001. Practical experiment designs: for engineers and scientists: John Wiley & Sons. https://books.google.com/books

[17] Liu H, Wang K, Schlindwein W, et al., 2013. Using the Box–Behnken experimental design to optimise operating parameters in pulsed spray fluidised bed granulation. Int. J. Pharm. 448: 329-338. https://doi.org/10.1016/j.ijpharm.2013.03.057

[18] D[1ewettinck K, Huyghebaert A, 1998. Top-spray fluidized bed coating: Effect of process variables on coating efficiency. LWT - Food Sci. 31: 568-575. https://doi.org/10.1006/fstl.1998.0417

[19] Eldeen, K. I., Ibrahim, H.M., Elkhidir, E. E., Elamin, H. B., "Optimization of culture conditions to enhance nattokinase production using RSM." American Journal of Microbiological Research. 3(5). pp. 165-170. 2015.

[20] Box GE, Hunter WH, Hunter S, 1978. Statistics for experimenters: John Wiley and sons New York.

[21] Vanaja K and Shobha Rani R., 2007. Design of experiments: concept and applications of Plackett Burman design. Clinical research regulatory affairs 24: 1-23. https://doi.org/10.1080/10601330701220520

[22] Seyedin Seyed Hadi, Zhalehrajabi Ehsan, Ardjmand Mehdi, et al., 2018. Using response surface methodology to optimize the operating parameters in a top-spray fluidized bed coating system. Surf. Coat. Technol. 334: 43-49. https://doi.org/10.1016/j.surfcoat.2017.11.003

[23] Bebs T, Roetzel W, 1992. Distribution of heat flux density in spiral heat exchangers. Int. J. Heat Mass Transf. 35: 1331-1347. https://doi.org/10.1016/0017-9310(92)90026-O

[24] Bes T, Roetzel W, 1998. Effectiveness of spiral heat exchanger with variable overall heat transfer coefficient. Heat Transfer and Renewable Energy Sources, Proc. VII Int. Symp. Heat Transfer and Renewable Energy Sources, Szczecin-Swinoujscie, Sept. 7-9.

[25] Bes T, Roetzel W, 1993. Thermal theory of the spiral heat exchanger. Int. J. Heat Mass Transf. 36: 765-773. https://doi.org/10.1016/0017-9310(93)80052-V

[26] Mostafa MA, 2011. Fouling of heat transfer surfaces. Heat Transfer-Theoretical Analysis, Experimental Investigations Industrial Systems, Prof. Aziz Belmiloudi , InTech.

[27] Červenka B, Holubčík M, Drga J, et al., 2022. Modular Spiral Heat Exchanger Thermal Modelling. Appl. Sci. 12: 5805. https://doi.org/10.3390/app12125805

[28] Bes T, 2001. Thermal design of spiral heat exchanger. Int. J. Heat. Exch. 2: 59-96.

[29] Kumar TA, Sharma N, Mohammad MN, et al., 2019. Optimization of spiral plate heat exchanger by gradient based optimizer. Int J Innov Technol Explor Eng 8: 1819-1823. ISSN: 2278-3075

[30] Liu Q, Tao Y, Shi L, et al., 2023. Parametric optimization of a spiral ground heat exchanger by response surface methodology and multi-objective genetic algorithm. Appl. Therm. Eng. 221: 119824.